Earth Planet. Sci. Lett. 653 (2025) 119224

Contents lists available at ScienceDirect

Earth and Planetary Science Letters

journal homepage: www.elsevier.com/locate/epsl

Uncovering the xenon isotope composition of continental rift magmas: Insight from analysis of geothermal gases at Homa Hills, Kenya

B. Marty [a,*], D. Contamine [a,b], D.V. Bekaert [a], A. Lastes [a], R. Pik [a], J. Labidi [c], E.D. Young [d], M.W. Broadley [e], P.H. Barry [f], D.J. Byrne [g], A.M. Seltzer [f]

[a] Université de Lorraine, CNRS, CRPG, 54000 Nancy, France
[b] ISTeP - Sorbonne Université, 4 Place Jussieu, 75252 Paris Cedex 05 France
[c] Université de Paris, Institut de Physique du Globe de Paris, CNRS, Paris, France
[d] Department of Earth, Planetary, and Space Sciences, UCLA, Los Angeles, CA, United States
[e] Department of Earth and Environmental Sciences, University of Manchester, Manchester, United Kingdom
[f] Marine Chemistry and Geochemistry Department, WHOI, 02543 Woods Hole, MA, United States
[g] Wairakei Research Centre, GNS Science, 114 Karetoto Road, Taupo 3377, New Zealand

ARTICLE INFO

Keywords:
Noble gases
Xenon isotopes
CO2-rich gases

ABSTRACT

We investigated geothermal gases from Homa Hills, a carbonatitic complex situated along an adjacent branch of the Kenyan rift system, using neon, argon, krypton, xenon and nitrogen isotopes. Large quantities of gas were sampled in Giggenbach-type bottles (Giggenbach, 1975) and analyzed by dynamic mass spectrometry to resolve isotopic variations at high precision (0.01-0.1‰; Seltzer and Bekaert, 2022; Bekaert et al., 2023; 2024). Neon and nitrogen isotope compositions are consistent with parental magmas being derived from the convecting mantle. Xenon isotopic data present ubiquitous enrichments (relative to air) of ^{129}Xe from the decay of extinct ^{129}I ($T_{1/2}$ = 15.7 Myr) and $^{131\text{-}136}Xe_f$ from fissions of ^{238}U ($T_{1/2}$ = 4.468 Myr) and/or ^{244}Pu ($T_{1/2}$ = 82 Myr). We also find slight excesses of ^{128}Xe (relative to ^{130}Xe and air), which could be due to subsurface isotopic fractionation during e.g., diffusive transport fractionation (DTF) and gravitational settling. However, the ^{128}Xe excesses are not accompanied by correlated Kr isotope excesses and plot off the empirical fractionation line defined from several other locations worldwide (Bekaert et al., 2023). Instead, a detailed isotope deconvolution suggests the occurrence of either chondritic Xe (with mantle ^{130}Xe consisting of up to 22 % of chondritic ^{130}Xe) or recycled Xe from the Archean atmosphere could explain the observed Xe isotope signatures. The latter possibility would have profound implications for models of mantle-surface exchange throughout Earth history.

The fission spectra indicate a predominantly ^{238}U origin for fissiogenic Xe, with contribution of ^{244}Pu-derived Xe being negligible within uncertainties, implying extensive mantle degassing during the Hadean and Archean eons. The ^{129}Xe*/^{136}Xe* ratio (where * indicates non-atmospheric excesses of Xe isotopes) of Homa Hills samples correlates with other tracers of mantle/crust contributions such as He, Ar and N isotopes. Variations in ^{129}Xe*/^{136}Xe* among the different gases sampled at Homa Hills is mainly the result of contribution from fissiogenic Xe produced in uranium-rich crustal material. Therefore, this ratio may constitute a robust tracer of mantle-crust interactions. Given available high precision data (Bekaert et al., 2023; 2024; this work) together with mantle-derived rock data, ^{129}Xe*/^{136}Xe* appears homogenous in the convecting mantle, and comparable to values observed at mantle plumes. Such homogeneity is in sharp contrast with light noble gas systematics and may call for whole mantle convection and a core origin for He and Ne..

1. Introduction

Noble gases are chemically inert and several of their isotopes are produced by time-dependent nuclear reactions, which make them excellent tracers of Earth's formation and evolution processes. Xenon is of particular interest since some of its isotopes were produced by extinct radionuclides: ^{129}Xe was produced during the first tens of Myr (after the start of solar system formation) by the decay of ^{129}I (half-life of 15.7

* Corresponding author.
E-mail address: bernard.marty@univ-lorraine.fr (B. Marty).

https://doi.org/10.1016/j.epsl.2025.119224
Received 11 September 2024; Received in revised form 14 January 2025; Accepted 15 January 2025
Available online 21 January 2025
0012-821X/© 2025 The Author(s). Published by Elsevier B.V. This is an open access article under the CC BY license (http://creativecommons.org/licenses/by/4.0/).

Myr), and the heavy Xe isotopes ($^{131\text{-}136}$Xe) were produced by the fission of ^{244}Pu (half-life of 82 Myr) during the first ~0.6 Gyr. These daughter isotopes were sequestered into the mantle and their abundances have subsequently varied due to mantle melting and degassing. Furthermore, $^{131\text{-}136}$Xe isotopes have been continuously produced by the fission of ^{238}U (half-life of 4,468 Myr) over the geological history of Earth (Ozima et al., 1985; Ozima and Podosek, 2002; Yokochi and Marty, 2005; Péron and Moreira, 2018; Mukhopadhyay and Parai, 2019). Using these different radiogenic isotopes allows one to set robust constraints to be placed on the degassing history of the mantle through geological periods of time. In a closed system, the Xe fission products of ^{244}Pu (Xe_{Pu}) dominate those of ^{238}U (Xe_U) by one order of magnitude, assuming a chondritic composition of refractory elements for the mantle (Pepin and Porcelli, 2006). However, mantle degassing through time depleted Xe_{Pu} while Xe_U continued to be produced. Hence the present-day mantle Xe_{Pu}/Xe_U ratio as well as the ^{129}Xe*/(Xe_{Pu}+Xe_U) ratio (where ^{129}Xe* denotes ^{129}Xe in excess of the atmospheric composition produced by the decay of ^{129}I) ratio are a function of kinetics and of the extent of mantle degassing. Early degassing during the first hundreds of Ma would deplete the mantle in Xe_{Pu}, and further production of Xe_U would result in a low Xe_{Pu}/Xe_U ratio, whereas protracted degassing would deplete both Xe_{Pu} and Xe_U. However, one difficulty is distinguishing the respective Xe isotope products of ^{244}Pu and ^{238}U, since the fission of both radionuclides produces the same $^{131\text{-}136}$Xe isotopes (Ozima and Podosek, 2002). Fortunately, the respective fissiogenic $^{131\text{-}136}$Xe spectra of ^{244}Pu and ^{238}U fission are slightly different, and the precise analysis of heavy Xe isotope compositions may allow one to estimate the nature of their fissiogenic parents. This problem has been discussed in numerous studies of rocks and minerals derived from the convective mantle or from mantle plume sources (Kunz et al., 1998; Moreira et al., 1998; Yokochi and Marty, 2005; Mukhopadhyay, 2012; Bekaert et al., 2019). Although excesses of ^{129}Xe from extinct ^{129}I are easily observed since it is a mono-isotopic signal, deciphering the origin of fissiogenic $^{131\text{-}136}$Xe isotopes from either ^{244}Pu or ^{238}U requires a precision at the permil (‰) level in volcanic rocks.

Noble gases in mantle derived rocks are always present in very low concentrations (order femtomole/g or less), and noble gases are classically analyzed by static mass spectrometry (SMS), in which standard and sample gases are sequentially analyzed. Recently, the analysis of noble gases by dual-inlet dynamic mass spectrometry (DMS) has been developed for volcanic and geothermal gases (Seltzer and Bekaert, 2022; Bekaert et al., 2023; 2024). This technique, which has long existed for conventional analysis of major gases in air (N_2, O_2), involves continuous flow from both a sample and reference gas, alternating every few seconds between analysis of each gas. While DMS enables noble gas isotope measurements at much higher precision than SMS, the drawback of this method is that it requires large amounts of noble gases, several orders of magnitude higher than those trapped in rocks typically measured by SMS. Naturally occurring gases have the potential to provide unlimited amounts of noble gases, but they also contain large quantities of major species like CO_2, H_2O and S-species, necessitating the efficient removal of these major chemical species prior to analysis. Noble gases and nitrogen gas can be concentrated in the field within an evacuated volume containing an alkaline solution that can trap CO_2, sulfur species and water vapor (Giggenbach, 1975; 1980; Bekaert et al., 2019; Bekaert et al., 2023). This method is particularly efficient for mantle-derived gases which are dominated (>99%) by CO_2 (Marty et al., 2020). DMS can achieve precision on the orders of 0.01-0.1 ‰ for Ar, Kr and Xe stable isotopic ratios (Seltzer and Bekaert, 2022; Bekaert et al., 2023; 2024). With such an improvement in precision, deconvolution of fissiogenic Xe isotopes becomes straighforward, and can now be applied to numerous degassing sites worldwide.

Interpreting noble gas isotope measurements in volcanic gas samples requires careful consideration to overcome two important challenges. Firstly, geothermal and volcanic gases are always affected by contribution of atmospheric noble gases due to interactions with subsurface water. As a result of this process, it has historically been quite rare to find gases in which mantle noble gases other than primordial helium can be detected at the precision of SMS (Butler et al., 1963). Secondly, naturally occurring gases experience complex interactions with the crust and/or groundwater that can induce isotope fractionation, potentially affecting the original mantle isotope composition (Nagao et al., 1979; Marty, 1984; Bekaert et al., 2023). To overcome these critical issues, a recent survey of global volcanic gas samples, analyzed via DMS, presented an approach of using Kr or Ar isotopes to correct for fractionation of Xe isotope, yielding robust constraints on mantle-derived Xe isotopes from a broad range of volcanic gas samples (Bekaert et al., 2023).

The ^{40}Ar/^{36}Ar of naturally occurring gases provides a robust index of atmospheric contribution to volcanic gas samples, since the mantle ratio (≥ 5,000, Moreira et al., 1998; Marty et al., 1998; Mukhopadhyay and Parai, 2019) is drastically different from the atmospheric ratio (298.6; Lee et al., 2006). Bekaert et al. (2024) reported DMS data for Eifel (^{40}Ar/^{36}Ar up to 10,000) and Etna (1900) gases. They found that the fractions of primordial Kr-Xe from accretionary sources and ^{244}Pu-derived ^{136}Xe are both lower than previously estimated. In order to document mantle heterogeneities, more data are required from different geodynamic settings.

Here we report noble gas data from Homa Hills geothermal gases, Kenya, an adjacent rifting zone of the East African Rift (EAR) system. In a noble gas survey of geothermal gases along the Kenyan rift, Darling et al. (1995) noted that most argon isotopic ratios of the sampled gases were close to the atmospheric composition, except at Bala, a bubbling hot spring in the Homa Hills region (Fig 1), for which they reported a ^{40}Ar/^{36}Ar ratio of 846, together with a ^{3}He/^{4}He ratio of 1.5 Ra (where Ra is the atmospheric value of 1.39×10^{-6}). Three hot spring gases in the Homa Hills region were sampled for high precision noble gas analysis and for nitrogen isotopologue analysis (Labidi et al., 2020; Labidi and Young, 2022). These gases presumably share a common magma source, but they have experienced variable contribution from the underlying Archean crust on one hand, and physical fractionation to different extent on another hand, allowing one to document not only the mantle source composition but also secondary processing during the transfer of gases from the mantle.

1.1. Geological setting, sampling and analytical procedures

The Homa Hills form an ensemble of carbonatitic centers that erupted from the Miocene to the Pleistocene. Four carbonatitic centers align along a regional fault that limits the graben of the Nyanza rift to the SW. The rift intersects neoArchean terranes of the Tanzanian Craton consisting of metavolcanics and granite intrusions dated between 2.8 and 2.5 Ga (Japan International Cooperation Agency Report, 1990). The Homa Hills are located south of the Kisumu city across the terminal Eastern extension of the Victoria Lake. They sit above the Archean Nyanzian (2.8 Ga) and Kadirondian (≥ 2.5 Ga) formations. Three hot spring sites, from North to South (Fig. 1), Ayombo, Abundu and Bala (also labelled Balla or Kakdimbu in the literature) discharge geothermal waters with maximum temperatures of 46.1 °C (Ayombo), 81.0 °C (Abundu), and 73.5 °C (Bala), respectively (Table 1). The fluids are alkaline saline sodium bicarbonate-chloride waters (Tole, 1988). Quartz geothermometry gives reservoir temperatures in the range 142-179°C while Na-K-Ca geothermometry suggests higher temperatures in the range 200-314 °C (Tole, 1988). The heat source could be related to shallow magmatic intrusions as shown by the occurrence of dikes that lie in-trend with the rift floor faults (Japan International Cooperation Agency Report, 1990).

The three sites had abundant bubbling gas that was sampled during a field trip funded by the EU-supported "Geothermal village" project (https://www.leap-re.eu/geothermal-village/) aimed to introduce geothermal-based stand-alone electric and thermal energy systems to off-grid African communities. The overall results and geothermal implications will be discussed elsewhere (Contamine et al., in prep.). In this

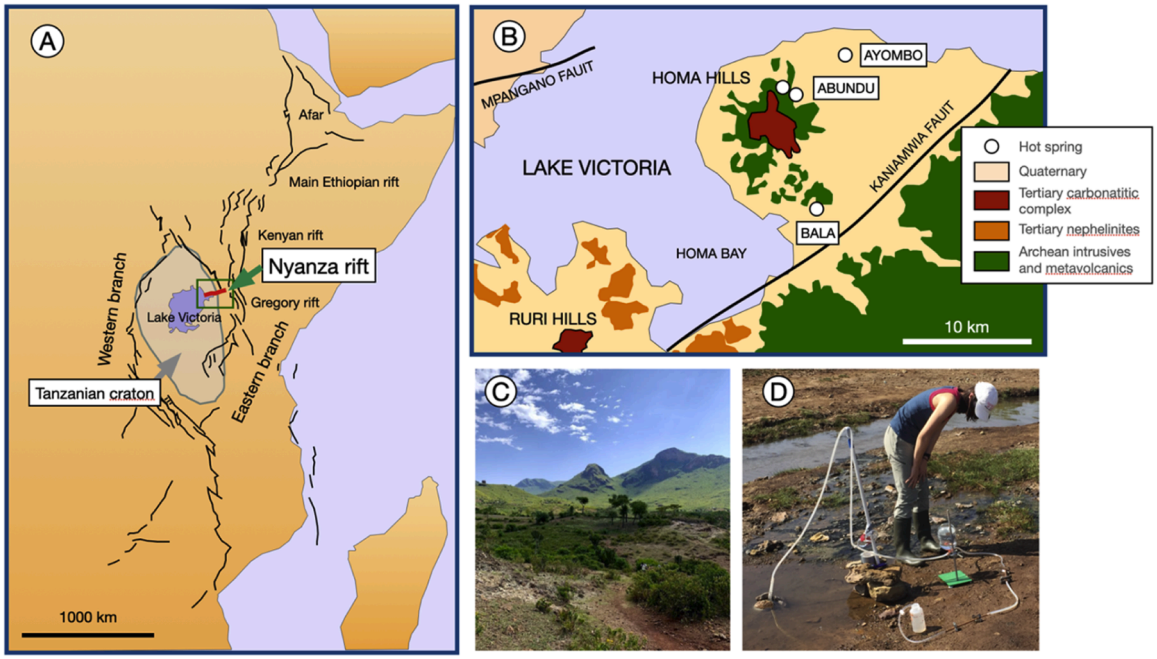

Fig. 1. (A): Simplified map of rifting in Eastern Africa, after Chorowicz (2005). The Nyanza rift is a branch of the Gregory Rift in Kenya that extents rifting towards West to the Lake Victoria. It intersects the Tanzanian craton consisting mostly of meso- to neoArchean volcanic and intrusive rocks (approximate contour from Foley et al., 2012). (B): Simplified geological map of the Homa Hills area on the eastern shore of Lake Victoria, after (Japan International Cooperation Agency Report, 1990). Homa Hills consists in a complex of carbonatitic rocks intruding neoArchean terranes. It lies with the Nyanza graben delineated SE of Homa Hills by major faults, here the Kaniamwia fault and escarpment SE of Homa Hills. The area includes four carbonatitic complexes of Miocene to Pleistocene ages. Bubbling gases were sampled at hot springs at Ayombo NE of Homa Hills, at Abundu 1 and 2 at the N foot of the hills, and at Bala. (C): A view on Homa Hills taken from the NE. (D): Gas sampling train at Ayombo spring. Bubble gas collected through a funnel were trapped in series in small Giggenbach bottles for chemical analysis and He, N_2 isotopes, in large 1 L Giggenbach bottle and in copper tubes for long-term conservation of helium isotopes.

Table 1
location of springs, water temperatures, nitrogen and neon isotopic data.

	Unit	Ayombo A	Ayombo B	Abundu 1A	Abundu 1B	Abundu 2A	Bala A	Bala B
Coord.	Decimal	-0.338762	-0.339290	-0.355205	-0.355205	-0.340991	-0.439504	-0.439504
Coord.	Decimal	34.539896	34.540938	34.510236	34.510236	34.538792	34.525166	34.525166
Temp.	°C	41.6	46.1	81.0	43.7	78.2	73.5	60.0
$\delta^{15}N$	‰/atm		-1.3	-0.9	-0.9		0.4	0.0
Δ_{30}	‰/stochastic		12.3	9.4	8.8		9.0	8.7
1 se Δ_{30}			0.1	0.2	0.2		0.3	0.1
$^{20}Ne/^{22}Ne$			9.939	10.226		10.229	10.184	
$\pm1\sigma$			0.026	0.085		0.088	0.089	
$^{21}Ne/^{22}Ne$			0.03113	0.03253		0.03181	0.03252	
$\pm1\sigma$			0.00050	0.00034		0.00037	0.00033	

contribution, we focus on noble gas data obtained at the Centre de Recherches Pétrographiques et Géochimiques (CRPG, Nancy, France), and high precision Ar, Kr and Xe isotope ratios measured at in the Seltzer Lab at Woods Hole Oceanographic Institution (WHOI) (Seltzer and Bekaert, 2022). Bubbling gas was collected at the three sites through a funnel into several Giggenbach-type bottles of 0.25 L (for chemistry, noble gases and nitrogen isotopes) and of 1 L (for DMS analysis), respectively. Upon arrival at CRPG, free gases were rapidly expanded into metal bottles fitted with double all-metal valves, and the CO_2, He, Ar and N_2 contents were measured by titration, volumetry, and mass spectrometry, respectively (chemical data to be reported elsewhere, Contamine et al, in prep.). The He and Ne isotopic ratios were measured by SMS on three mass spectrometers including a split flight tube for helium isotopes (Mabry et al., 2013). We report here and discuss high precision analysis of Ar, Kr and Xe together with new neon isotope data and nitrogen isotopologue data (Labidi et al., 2020).

2. Results

Table 1 displays hot spring coordinates, water temperature, nitrogen and neon isotope data. Ar, Kr and Xe abundances and isotopic ratios, analyzed by dynamic mass spectrometry (DMS), are given in Table 2.

2.1. Helium, neon and argon

He isotope values are 1.63 R_a for Bala, 2.21 R_a for Abundu and 2.55 R_a for Ayombo, where R_a is the atmospheric $^3He/^4He$ ratio of 1.39×10^{-6}; Mamyrin and Tolstikhin, 1984). The $^3He/^4He$ ratio is consistently lower than known mantle end-members suggesting radiogenic helium (^4He) was incorporated into the gas, presumably from the underlying Archean

Table 2
Dynamic mass spectrometry (DMS) data for noble gas elemental and isotopic abundances. The $^{40}Ar/^{36}Ar$ are absolute values, while other values are given in ‰ relative to their respective atmospheric compositions.

Sample	$^{40}Ar/^{36}Ar$	±1 σ	$\delta^{84}Kr/^{36}Ar$	$\delta^{132}Xe/^{36}Ar$	$\delta^{86/84}Kr$	±1 σ	$\delta^{82/84}Kr$	±1 σ
Ayombo A	778.62	0.23	2477	10230	0.164	0.018	-0.125	0.022
Abundu 1A-1	844.80	0.19	907	2633	-0.061	0.030	0.092	0.035
Abundu 1A-2	845.17	0.24	920	2678	-0.020	0.030	-0.003	0.035
Abundu 1A-3	845.12	0.25	921	2683	0.023	0.030	0.041	0.035
Bala A-1	950.69	0.52	975	2642	0.247	0.032	-0.204	0.038
Bala A-2	948.54	0.52	972	2632	0.286	0.032	-0.164	0.038
Sample	$\delta^{128/130}Xe$	±1 σ	$\delta^{129/130}Xe$	±1 σ	$\delta^{131/130}Xe$	±1 σ		
Ayombo A	0.159	0.109	5.148	0.050	0.187	0.061		
Abundu 1A-1	0.346	0.201	4.857	0.092	-0.030	0.113		
Abundu 1A-2	0.314	0.200	4.867	0.092	-0.054	0.113		
Abundu 1A-3	0.508	0.200	4.892	0.092	0.081	0.113		
Bala A-1	0.662	0.214	4.613	0.098	0.190	0.121		
Bala A-2	0.318	0.214	4.502	0.098	0.038	0.121		
Sample	$\delta^{132/130}Xe$	±1 σ	$\delta^{134/130}Xe$	±1 σ	$\delta^{136/130}Xe$	±1 σ		
Ayombo A	1.076	0.050	4.191	0.056	6.000	0.067		
Abundu 1A-1	0.938	0.092	4.245	0.104	5.909	0.125		
Abundu 1A-2	0.888	0.092	4.225	0.104	6.046	0.124		
Abundu 1A-3	0.962	0.092	4.305	0.103	6.073	0.124		
Bala A-1	1.412	0.098	5.563	0.111	7.868	0.133		
Bala A-2	1.314	0.098	5.439	0.111	7.873	0.133		

terranes (Contamine et al., in prep.). The neon isotopic ratios, measured at CRPG by static mass spectrometry, plot along the mid-ocean ridge basalt (MORB) correlation line and do not fall along mantle plume arrays, represented here by Icelandic data (Fig. 2). Neon isotope data are consistent with a magma source originating from the convecting mantle, even if the He isotopic ratios are richer in radiogenic ^{4}He than those observed along mid-ocean ridges. This contrasting trend could be related to the contribution of radiogenic helium diffusing out of the U, Th-rich Archean terranes intersected by the Kaniamwia fault through which magmatic gases make their way to the surface (see the Discussion section).

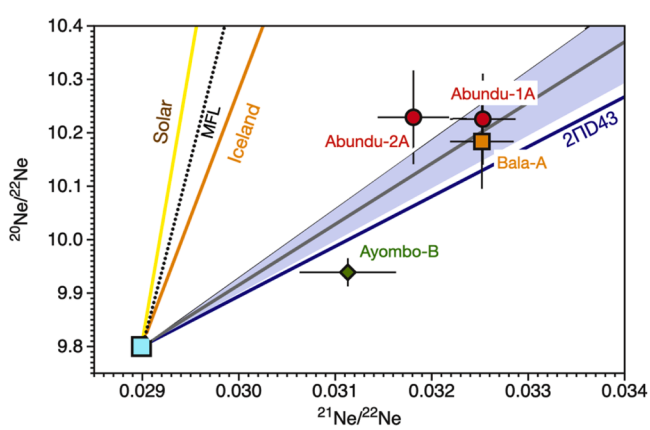

Fig. 2. Neon three-isotope diagram for Homa Hills samples. Errors are 1 σ. The dark blue line represents the MORB correlation defined by gas-rich sample 2ΠD43 (Parai and Mukhopadhyay, 2021), the Iceland line from Mukhopadhyay (2012) represents a typical mantle plume signature, and the yellow line connects the solar wind and atmosphere compositions, respectively, the dotted line labelled MFL represents Ne isotope evolution upon mass-dependent kinetic isotope fractionation (Young et al., 2002) and the light blue area represents the uncertainty on the linear regression of Homa Hills data (Total Least Square Model 2, Isoplot R; Vermeesch, 2018).

The $^{40}Ar/^{36}Ar$ values (Table 2) are 778 (Ayombo), 845 (Abundu) and 950 (Bala), significantly higher than the atmospheric value of 298.6, confirming the previous observation on Bala gas for which Darling et al. (1995) reported a $^{40}Ar/^{36}Ar$ of 846. The He isotope ratios show covariation with those of Ar, indicating increasing radiogenic isotope contribution from Ayombo to Bala. The latter is the site closest to the Kanianzia fault delineating the graben structure to the SE (Fig. 1) and intersecting the local Archean crust.

2.2. Nitrogen isotopes

We quantify the amounts of air-derived gases using the $^{15}N^{15}N$ approach (Labidi et al., 2020; Labidi and Young, 2022). We measured Δ_{30}, the relative proportion of $^{15}N^{15}N$ relative to a random distribution of ^{14}N and ^{15}N atoms among N_2 molecules, as a tracer of surficial atmospheric contamination. The Δ_{30} tracer is defined as $\Delta_{30} = {}^{30}R/({}^{15}R)^2$ - 1 (‰), where $^{30}R = {}^{15}N^{15}N/{}^{14}N^{14}N$ and $^{15}R = {}^{15}N/{}^{14}N$. At most temperatures relevant to geological processes, equilibrium among N_2 isotopologues results in Δ_{30} values between 0.1 and 0.5‰ (Yeung et al., 2017). This is the case of magmatic and crustal N_2, whether it is mantle-derived, inherited from a slab, or from shallow crustal reservoirs (Labidi et al., 2020; 2021). In contrast, air has a pronounced disequilibrium $^{15}N^{15}N$ enrichment, corresponding to an atmospheric Δ_{30} value of 19.1±0.3‰ (2σ; Yeung et al., 2017). We make use of this disequilibrium as a tracer for air contributions in natural fluids and identify the compositions of mantle sources for N_2.

The nitrogen isotopic composition was determined for five of the samples (Table 1, Fig. S2). The Δ_{30} values vary between 8.7 and 12.3‰, suggesting air-derived nitrogen contributes to ~40% to 60% of the N_2 in the samples, and the $\delta^{15}N$ values vary between -1.3 and 0.4‰. The samples with lower Δ_{30} of ~ 9‰ have slightly more elevated $\delta^{15}N$. In contrast, the sample with the most elevated Δ_{30} of 12.3‰ (Ayombo) has

the lowest $\delta^{15}N$ value of -1.3‰. These data could indicate the contribution of air-derived nitrogen with a fractionated $^{15}N/^{14}N$. Mass-dependent fractionation of air-derived nitrogen has been recently shown to commonly lead to negative $\delta^{15}N$ values in various springs and hydrothermal samples (Labidi et al., 2020, 2021), as the result of water/gas isotope fractionation in the subsurface (Labidi and Young, 2022). However, these data are also consistent with mixing of ~60% atmospheric N_2 with ~40% N_2 from the convective mantle having a $\delta^{15}N$ of -3‰ ~ -5 ‰ (Cartigny and Marty, 2013). There is no clear correlation with other indicators of atmospheric contamination such as the $^{40}Ar/^{36}Ar$ ratio, probably because there are several end-member components: both the mantle and the Archean crust present $^{40}Ar/^{36}Ar$ values higher than the atmospheric value. Nonetheless, Δ_{30} values of 9‰~12‰ require that a substantial amount of atmospheric nitrogen, with Δ_{30} values of 0‰, contributes to the springs. Consequently, N isotope data can be corrected for such atmospheric contribution using Δ_{30} values (see Fig. S2).

3. Discussion

The helium, neon, argon and nitrogen isotope ratios measured in Homa Hills gases are consistent with a three-component mixing of atmospheric (i.e., $^{40}Ar/^{36}Ar$ ratios lower than mantle or crustal values, $\Delta_{30} > 0$‰), mantle-derived (occurrence of primordial ^{3}He, MORB-like Ne and corrected N isotopes), and crustal ($^{3}He/^{4}He$ lower than air and MORBs) gases. CO_2-rich gases sampled at Homa Hills are among the least air-contaminated, mantle-derived gases sampled so far across the African continent, based on $^{40}Ar/^{36}Ar$ ratios (Darling et al., 1995; Aka et al., 2001; Fischer et al., 2009; Gilfillan et al., 2019). They provide a unique opportunity to investigate at high precision the noble gas isotope composition of the underlying mantle in a continental rift setting. Although $^{3}He/^{4}He$ values are lower than those sampled at mid-ocean ridges, the Ne isotopic signature of these gases point to a convective mantle domain as the source of Homa Hills magmas (Fig. 2). Another possibility would be a contribution of mantle plume material in some of the rifted area of Africa, as indicated by Ne isotopes (Halldórsson et al., 2014; Gilfillan et al., 2019). The addition of crustal Ne could potentially modify an initial plume-like Ne signature, resulting in the Ne isotope data being offset towards the MORB-air mixing line (Fig. 2). However, the three gases have variable crustal contribution according to Xe isotopes (see below) but still lie along the MORB correlation, suggesting limited contribution of nucleogenic ^{21}Ne from the crust. In particular, Ayombo presents a $^{129}Xe^*/^{136}Xe^*$ (where * means radiogenic and fissiogenic isotopes in excess of the atmospheric composition) ratio close to values defining the convective mantle (Fig. 8). In the following discussion, we examine in detail the isotopic composition of xenon, assuming that these gases are issued from the convecting mantle, with a potential crustal contribution from the overlying Archean-Proterozoic terranes.

3.1. Deconvolution of Xe components in the Homa Hills gases

One of the challenges of noble gas geochemistry is to establish whether different mantle domains (e.g., mantle plume regions, convective mantle) present specific proportions of parent nuclides that could be related to past geodynamics and degassing. For instance, Mukhopadhyay (2012) proposed that fissiogenic xenon in Icelandic glasses is dominated by Xe_{Pu}, in line with the presumably less degassed character of mantle plume sources compared to the convecting MORB mantle. For MORBs, inconsistent contributions of Pu to total fissiogenic Xe have been proposed, from Pu-dominated (Kunz et al., 1998; Moreira et al., 1998; Péron and Moreira, 2018) to U-dominated (Parai and Mukhopadhyay, 2021). In the following, we attempt to estimate the nature and history of mantle noble gases using primordial and secondary (radiogenic and fissiogenic) Xe isotopes.

Fig. 3 shows all Xe isotope data in the δ notation, including

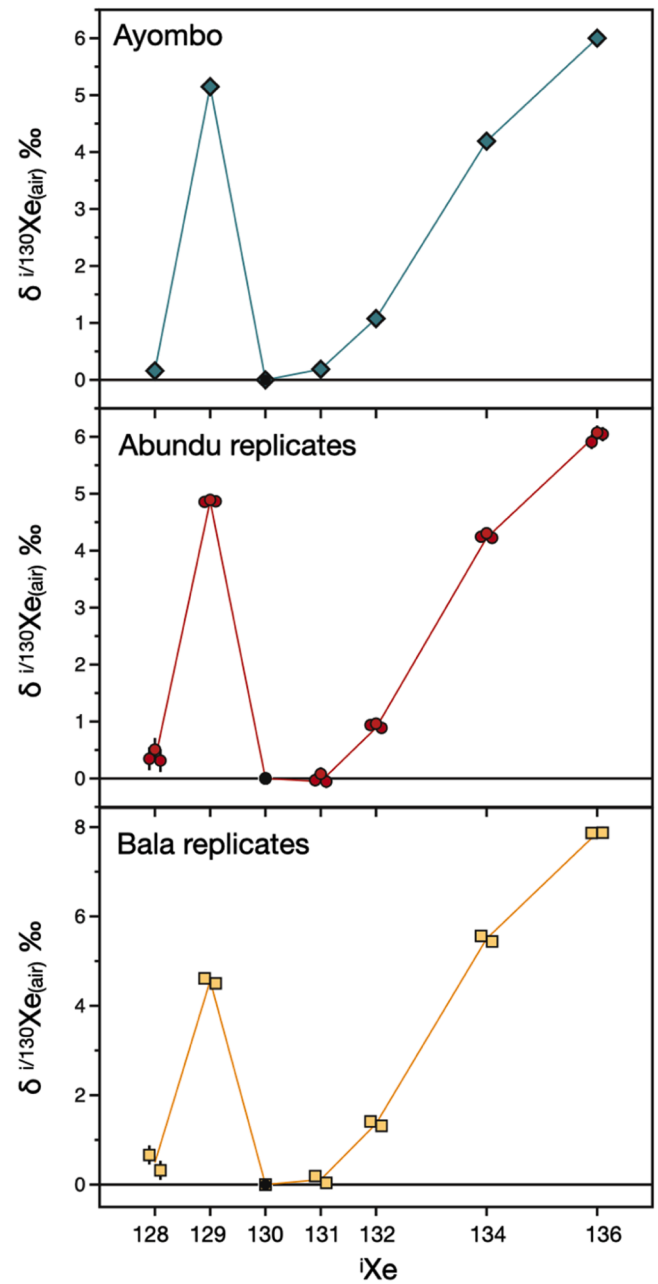

Fig. 3. Individual Xe data obtained by DMS (Data from Table 2).

duplicates for the three sites, with $\delta^{i/130}Xe = \left[\left(\frac{^{i}Xe}{^{130}Xe}\right)_{sample} / \left(\frac{^{i}Xe}{^{130}Xe}\right)_{air} - 1\right] \times 1000$, where the suffix air is the atmospheric Xe composition. All gases show clear excesses (i.e., positive delta values) in ^{129}Xe from the decay of extinct ^{129}I ($T_{1/2}$ = 15.7 Ma) and $^{131\text{-}136}Xe$ from fission of ^{238}U ($T_{1/2}$ = 4450 Ma) and/or extinct ^{244}Pu ($T_{1/2}$ = 82 Ma). These clear isotope excesses fully confirm a mantle origin for Homa Hills gases. However, the limited magnitude of these excesses compared to those of mantle-derived rocks shows that most of the Xe is atmosphere-derived. Taking for instance a $^{129}Xe/^{130}Xe$ of 7.41 for the convecting mantle end-member (Parai and Mukhopadhyay, 2021) and using the atmospheric $^{129}Xe/^{130}Xe$ value of 6.496 (Ozima and Podosek, 2002), one obtains a $\delta^{129/130}Xe$ value of 141‰ for the convecting mantle, to be compared with the $\delta^{129/130}Xe$ of around 5‰ for Homa Hills gases (Fig. 3). Hence the fraction of atmospheric Xe is > 96% (see Supplementary Materials

for calculation). Because noble gas isotope ratios are normalized to atmospheric values, the only uncertainties are those due to DMS measurements, so that typical errors of $\leq \sim 0.2‰$ permit to safely assess the composition of the mantle component, even at the $\geq$ 96% level contamination.

In order to investigate the primordial origin of Xe, only the isotopes not produced by radioactive or fissiogenic processes are relevant. This criterium eliminates ^{129}Xe from radioactive decay of ^{129}I, and $^{131\text{-}136}$Xe from fissions of ^{238}U and ^{244}Pu. Thus only ^{124}Xe, ^{126}Xe, ^{128}X and ^{130}Xe are considered as primordial isotopes (Ozima and Podosek, 2002). At present, the DMS method available at WHOI (Seltzer Lab.) has not yet been set up to measure the rare ^{124}Xe and ^{126}Xe isotopes, so only the ^{128}Xe/^{130}Xe ratio can be used here to explore primordial isotope systematics. The ^{128}Xe isotope is slightly in excess of the atmospheric composition (($\delta^{128/130}$Xe) > 0; Table 1 and Fig. 3) and this excess could reveal the occurrence of a primordial component in the mantle source, as observed in mantle-derived rocks (e.g., Mukhopadhyay and Parai, 2019, and refs. therein). Alternatively, it could primarily reflect isotope fractionation of atmosphere-derived Xe in subsurface fluids (Bekaert et al., 2023; 2024). With only one isotope ratio, the difference between these drastically different possibilities cannot be easily resolved and independent constraints are therefore needed.

Several processes fractionating noble gas isotopes (i.e., counter-diffusion of pore gases in a current of stream, gravitational settling) have been identified in subsurface hydrothermal systems (Bekaert et al. (2023). Bekaert et al. (2023) proposed to compare the excesses of ^{128}Xe ($\delta^{128/130}$Xe) to that of ^{86}Kr relative to ^{84}Kr ($\delta^{86/84}$Kr). The rationale is that the mantle composition of Kr is very close to that of atmospheric Kr, so that any deviation in Kr isotopes to the atmospheric composition would likely be due to physical fractionation. Péron et al. (2021) challenged this assumption by proposing that the mantle end-member has a $\delta^{86/84}$Kr value of $\sim +3‰$. However, Bekaert et al. (2024) only found minor (if any) heavy Kr isotope excess attributable to a chondritic component in Mt. Etna gases. These authors also found air-like $\delta^{86/84}$Kr for a CO_2-rich gas at Eifel having an unambiguous mantle signature (^{40}Ar/^{36}Ar = 10,177). Hence it is not clear yet whether mantle Kr has an isotopic composition markedly different from that of air. Most data for gases sampled worldwide display negative $\delta^{86/84}$Kr values (Bekaert et al., 2023; Fig. 4) attributed to diffusive transport fractionation (DTF) process. Noble gases from subsurface water or in soil porosity would counter-diffuse into a stream of CO_2, a process proposed by Marty (1984) to account for noble gas isotope fractionation observed in Kr and Xe by Nagao et al. (1979) in geothermal gases. Such a mass-dependent process suggests $\delta^{128/130}$Xe variations should anticorrelate with $\delta^{86/84}$Kr, given the respective isotope masses (i.e., $m_{86}>m_{84}$ vs. $m_{128}<m_{130}$). Bekaert et al., (2023) found that this is effectively the case for numerous hydrothermal gases sampled worldwide in contrasting geodynamic environments like mantle plumes, intraplate volcanism, and subduction zones (Fig. 4). These authors proposed an empirical method to correct for DTF: When the sample data points are seated on a correlation line between ^{128}Xe^{130}Xe and ^{86}Kr/^{84}Kr, then the slope of the correlation can be used to correct the Xe isotope composition (Bekaert et al., 2023). In the present case, the Homa Hills data points plot systematically above the worldwide correlation with ($\delta^{86/84}$Kr) close to zero for Abundu, and slightly positive values for Ayombo and Bala (Fig. 4). The latter could indeed reflect the occurrence of a mantle Kr component as proposed by Péron et al (2021). However, Abundu, which has a mantle source common to Ayombo and Bala, does not show positive ($\delta^{86/84}$Kr) value whereas all three gases are above the DTF correlation. We tentatively conclude that excesses of ^{128}Xe observed in Homa Hills gases may not result from isotope fractionation in subsurface fluids. Consequently, ^{128}Xe excesses could reflect the occurrence of either (i) a primordial component isotopically different from atmospheric Xe, or (ii) a Xe component being isotopically fractionated while associated Kr is not. We explore these two possibilities in the following subsection.

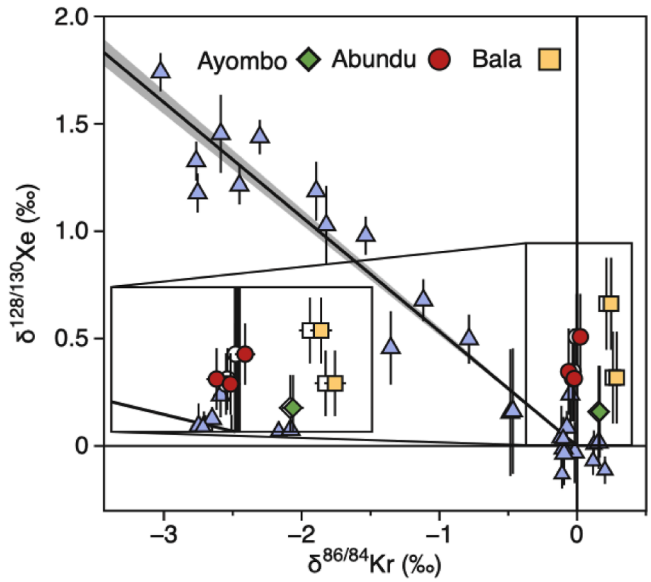

Fig. 4. Relationship between $\delta^{86/84}$Kr (deviations of the ^{86}Kr/^{84}Kr ratios relative to the atmospheric value in part permil) and $\delta^{128:130}$Xe (deviations of the ^{128}Xe/^{130}Xe ratios relative to the atmospheric value in part permil) for gases sampled worldwide (Bekaert et al., 2023). Subsurface mass-dependent isotopic fractionation (MDF) is expected to affect both Kr and Xe. The empirical correlation with a slope of -0.5331±0.0179 permits to correct Xe isotopes for diffusive transport fractionation (DTF). Samples from this study (all replicates shown here) do not show correlated $\delta^{86/84}$Kr - $\delta^{128/130}$Xe values, with $\delta^{128/130}$Xe being systematically above the correlation. The insert details Kenyan data, showing that the Abundu samples show no excess of ^{86}Kr while showing excesses of ^{128}Xe, but the Bala and to a lesser extent Ayombo samples show excesses of both ^{86}Kr and ^{128}Xe. The $\delta^{86/84}$Kr ratios were corrected for fissiogenic ^{86}Kr using excesses of fissiogenic ^{136}Xe (see Supplementary Materials for method). The corrected values, shown by open symbols, are close to the observed data.

3.2. Chondritic xenon in the mantle source(s)

In a first scenario, mantle Xe is considered to be the result of mixing between subsurface Xe and a primordial component acquired during Earth's formation. For the latter, a chondritic origin has been proposed based on the similarity between extrapolated mantle end-members (CO_2 well gases, Yellowstone and MORB) and the average carbonaceous chondrite (AVCC) composition (Holland et al., 2009; Broadley et al., 2020; Péron et al., 2021). The mantle Xe component itself is not purely primordial, but also contains a component akin of the atmospheric composition (Holland and Ballentine, 2006; Holland et al., 2009; Péron and Moreira, 2018; Parai and Mukhopadhyay, 2018; Mukhopadhyay and Parai, 2019). This possibility is substantiated by studies of noble gases in arc-related lithologies (Sumino et al., 2010; Kobayashi et al., 2017) and volatile budgets at arcs (Bekaert et al., 2021). All of these studies call for efficient subduction of heavy noble gases back to the convective mantle. The fraction of recycled atmospheric xenon either in the convecting mantle feeding mid-ocean ridges or in the plume-influenced mantle sources has been estimated to be ~80-97% (Parai and Mukhopadhyay, 2021; Bekaert et al., 2024). The primordial krypton and xenon isotopic compositions are not well known, and, in the absence of contrary evidence, we assume an AVCC composition for non-atmospheric Xe in the magma source of Homa Hills.

We tentatively correct the observed Xe isotope ratios for this AVCC contribution using a two-steps process (see Supplementary Materials). First, we assume binary mixing between a convecting mantle end-member characterized by a ^{129}Xe/^{130}Xe of 7.41±0.02 (Parai and Mukhopadhyay, 2021) and surface atmospheric Xe (^{129}Xe/^{130}Xe = 6.496), with the amount of AVCC gas being solely constrained by the

^{128}Xe excesses relative to the atmospheric composition. This allows us to compute the ^{128}Xe/^{130}Xe ratio of mantle Xe after correction for surface atmospheric Xe. Secondly, we assume that mantle Xe is itself a mixture of subducted atmospheric Xe and AVCC-like Xe. The fractions of AVCC in the mantle sources of Homa gases are computed to be 15.7±10.5 %, 22.5±15.2 % and 6.4±4.2 % for the mantle sources of Abundu, Bala and Ayombo, respectively, the rest being subducted atmospheric Xe (Supplementary Materials). Such estimates are consistent with those found in the literature (Parai and Mukhopadhyay, 2021; Bekaert et al., 2024; and references therein). Compared to atmospheric Xe, AVCC Xe is depleted in the heavy Xe isotopes relative to the light ones. Therefore, subtracting the AVCC isotopes progressively increases the ^{i}Xe/^{130}Xe ratios according to their increasing masses. In particular, the ^{129}Xe*/^{136}Xe* ratios will be lowered following this correction (Figs. 5 and S1).

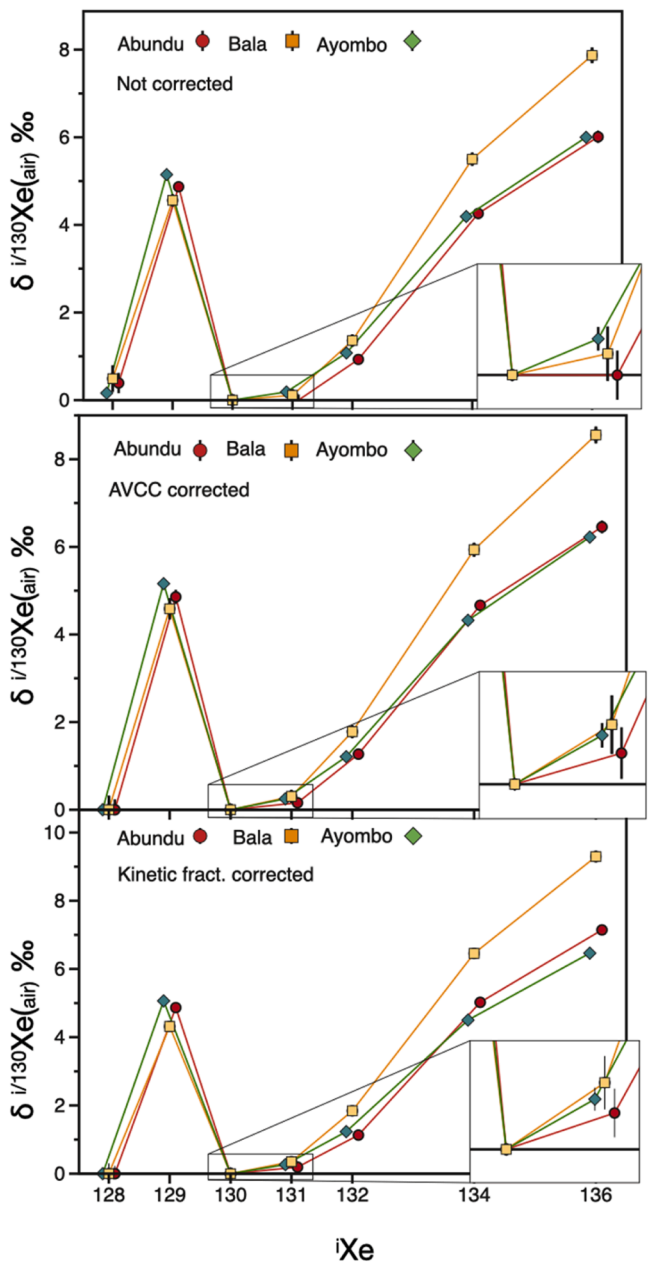

Fig. 5. effects of corrections on the Xe isotope spectra (from top to bottom: original data, AVCC corrected and kinetic isotope fractionation corrected). Xe masses are slightly shifted for better visualization.

3.3. Fractionated ancient atmospheric xenon in the mantle source(s)?

In a second scenario, mantle Xe is considered to be isotopically fractionated while Kr is not. It is difficult to envision a mantle or surface process that would fractionate xenon only, but such a process might have taken place in the past. Atmospheric xenon is isotopically fractionated by 3.6%/u compared to any cosmochemical progenitor (Ozima and Podosek, 2002; Pepin, 2006). The analysis of paleo-atmospheric samples from the Archean eon showed that ancient xenon had an isotopic composition intermediate between cosmochemical Xe and modern atmospheric Xe (Pujol et al., 2011), and that this difference evolved with time during the Archean period (Avice et al., 2017; Avice et al., 2018; Broadley et al., 2022), to reach the modern-like atmospheric composition around the Archean-Proterozoic transition (Ardoin et al., 2022). This evolving Xe isotope fractionation was attributed to xenon escape to space while other noble gases remained in the atmosphere. Preferential Xe escape was likely due to its low ionization potential (Hébrard and Marty, 2014; Zahnle et al., 2019), which might have been dragged by escaping hydrogen ions (Zahnle et al., 2019). This process provides a natural way to isotopically fractionate Xe isotopes without fractionating other noble gases (Zahnle et al., 2019), including Kr. Parai and Mukhopadhyay (2018) used the isotopic evolution of atmospheric Xe to build a model of mantle-atmosphere exchange of volatile elements, concluding that recycling of water and other volatiles was not efficient before the Archean-Proterozoic transition around 2.4 Ga.

Here we test the possibility that recycling of atmospheric Xe, which resulted in ≥ 80 % mantle Xe being recycled atmospheric Xe (see above), was already taking place before the end of Xe isotopic evolution at 2.4 Ga, so that excesses of ^{128}Xe could be due to mantle Xe containing a contribution of an ancient (Archean) atmospheric component. The fractionation process is highly model-dependent (Zahnle et al., 2019), and, for the purpose of demonstration, we postulate kinetic fractionation, where three isotopes 1, 2, 3 fractionate according to:

$$\alpha_{2/1} = \alpha_{3/1}{}^{\beta} \tag{1}$$

with a fractionation factor β equal to (Young et al., 2002):

$$\eta = \frac{ln\left(\frac{m_1}{m_2}\right)}{ln\left(\frac{m_1}{m_3}\right)} \tag{2}$$

There are several possibilities for defining the η factor, including the reduced mass of the system, or the involvement of a major gas species such as CO_2 (Bekaert et al., 2023), H_2O or N_2 for diffusion in the atmosphere, and kinetic isotope fractionation may represent an upper limit for the extent of MDF (Severinghaus et al., 1996). To correct for the contribution of this component, we assign a value of 0 for $\delta^{128/130}$Xe and compute the fractions of isotopically fractionated $^{129,131\text{-}136}$Xe with the above fractionation law (Fig. 5, bottom). These fractions are then removed from the observed isotopic ratios. As for the AVCC correction, the ^{129}Xe*/^{136}Xe* ratio is lowered following this operation.

3.4. Nature of fissiogenic Xe in Homa Hills gases

The AVCC (first scenario) and kinetic fractionation (second scenario) corrections on the bulk Xe spectra show enhancements of $^{131\text{-}136}$Xe isotopes that fit better than those expected for production by fission of either ^{238}U or ^{244}Pu. The effects of corrections are highlighted in Fig. 6, which represents the ^{i}Xe*/^{136}Xe* ratios, where i stands for 131, 132 or 134 and * stands for fission production from either ^{244}Pu or ^{238}U. Fig. 6a represents the original data, for which fission spectra do not adequately reproduce the fissiogenic patterns for ^{238}U and ^{244}Pu. Fig. 6b (second scenario) shows the data corrected for contribution of isotopically fractionated atmospheric xenon, as expected for mantle Xe being contributed by ancient atmospheric xenon. Fig. 6c represents a third

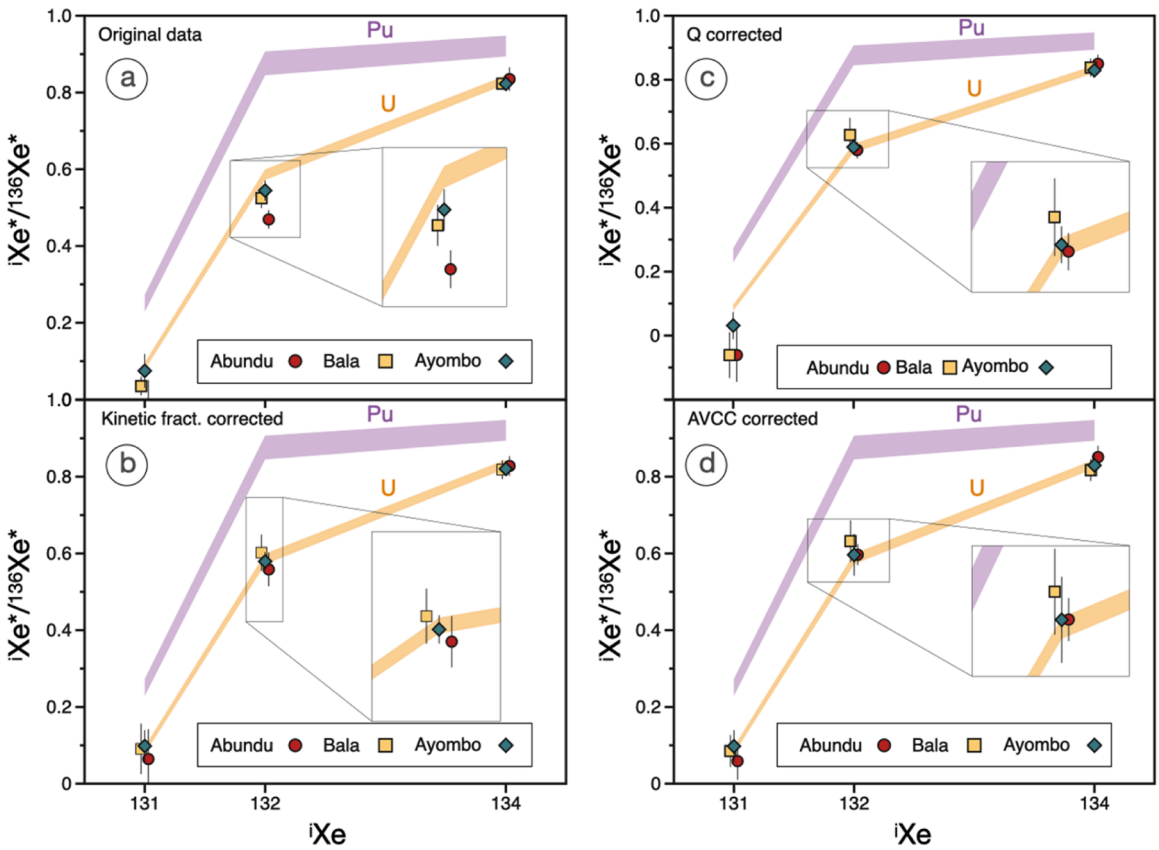

Fig. 6. Ratios between heavy Xe isotope excesses normalized to ^{136}Xe*, where * stands for fissiogenic. Data masses are slightly shifted for better visualization. a: original data; b: corrected for kinetic isotope fractionation; c data corrected for Q contribution; d: data corrected for contribution of AVCC. The fission spectra for ^{244}Pu (purple color) and for ^{238}U (beige color) are given for comparison. Error bars are 1 σ.

scenario, in which the primordial component of mantle Xe is assumed to be of Q-type Xe, a ubiquitous component found in non-carbonaceous chondrites such as enstatite chondrites (EC). This possibility is based on mantle volatiles (e.g., water and nitrogen) originating from EC-like material (Piani et al., 2020). The fit in this case is poor since the ^{131}Xe*/^{136}Xe* values are too low compared to either ^{244}Pu or ^{238}U fission spectra, however we include it for completeness. Fig. 6d (scenario one) assumes that xenon in the mantle originated from carbonaceous chondrites (AVCC; Mazor et al., 1970; Péron et al., 2021). Both corrections for kinetic fractionation or for AVCC contribution yield satisfactory fits, which are more consistent with ^{238}U fission, rather than ^{244}Pu. This observation is in line with previous conclusions by Bekaert et al. (2023; 2024) that the potential contribution of ^{244}Pu to fissiogenic Xe is much lower than previously assumed from static mass spectrometry studies (Kunz et al., 1998; Moreira et al., 1998; Yokochi and Marty, 2005; Mukhopadhyay, 2012; Bekaert et al., 2019).

In detail, data from Bala corrected for AVCC contribution (Fig. 6d and Fig. 7), may allow a limited contribution of ^{244}Pu. However, because the gases from these three hot springs are thought to be derived from a common magma source, variable additions of fissiogenic Xe (Fig. 6) are likely the result from the contribution of ^{238}U fission from the underlying Archean crust (see next subsection). Notably the Bala gas contains more fissiogenic Xe (e.g., ~30 % higher ^{129}Xe*/^{136}Xe* ratio than the two other gases; Fig. 4), as well as higher radiogenic (^{4}He, ^{40}Ar) isotope contributions than the two other samples (Table 1), so this sample should have an even larger Xe_U contribution than Abundu and Ayombo. To have a significant contribution of ^{244}Pu in Bala gas is, therefore, unlikely.

The best fit of fissiogenic data is obtained by assuming contribution of kinetically fractionated atmospheric Xe (Figs. 6 and 7) and this possibility may have far-reaching implications for the origin of mantle volatiles. It would imply that there is no discernable remnant of primordial (i.e., non-atmospheric) xenon and that the mantle Xe budget has been overprinted by Xe that was once at the surface of the Earth. The isotope composition of this atmospheric component appears mostly modern-like, consistent with Xe recycled at periods of time younger than 2.4 Ga, but traces of isotopically fractionated Xe may also indicate that recycling of paleo-atmospheric Xe already took place before 2.4 Ga, i.e., during the Archean (or Hadean) eon. A critical test of this possibility will require analyzing the rare isotopes of ^{124}Xe and ^{126}Xe at high precision when technical developments permit.

3.5. *The $\delta^{129/136}$Xe ratio as a tracer of mantle geodynamics*

We investigate here the potential of the ratio between radiogenic/fissiogenic excesses, i.e., ^{129}Xe*/^{136}Xe* or $\delta^{129/130}$Xe/$\delta^{136/130}$Xe, written in the following as $\delta^{129/136}$Xe, as a tracer of degassing and mantle dynamics. ^{129}Xe* was generated early from the decay of ^{129}I and, since its production ceased within the first ~100 Ma, its mantle abundance subsequently varied only by magma generation and degassing. ^{129}Xe* may therefore be considered as a "primordial" isotope like, e.g., ^{3}He. Likewise, ^{136}Xe* production via ^{244}Pu fission only occurred during the first ~0.6 Ga of Earth evolution, while ^{238}U fission was still ongoing today. The fact that fissiogenic Xe* in the mantle is now dominated by Xe_U (Fig. 7) is clear evidence for extensive degassing by convection and crustal production during the Hadean and Archean eons (Coltice et al., 2009; Bekaert et al., 2024). Indeed, ^{244}Pu was present in chondrites (Hudson et al., 1989) and Xe_{Pu} was found in chondritic proportions relative to U in Hadean zircons (Turner et al., 2007). Bekaert et al. (2024) proposed that Pu was extracted from the mantle to the Hadean crust and fissiogenic Xe was subsequently degassed into the Hadean atmosphere while U was recycled back into the mantle. Early crustal

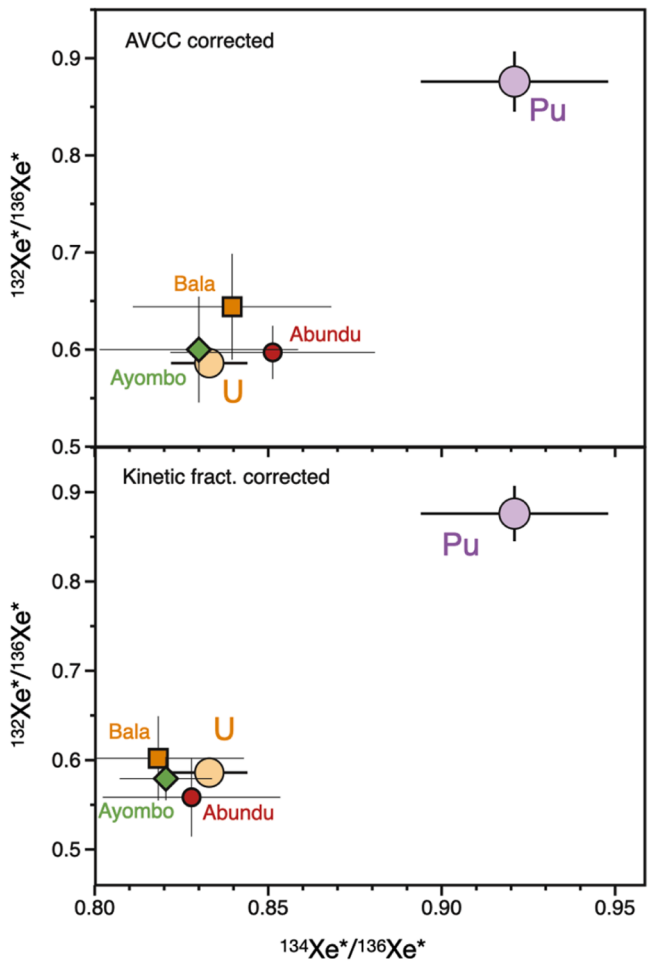

Fig. 7. ^{132}Xe* vs. ^{134}Xe* normalized to ^{136}Xe*, where * stands for fissiogenic. From top to bottom: data corrected for AVCC contribution and data corrected for contribution of atmospheric xenon fractionated by kinetic isotope fractionation. The fission ratios of ^{244}Pu (Alexander et al., 1971; purple dot) and for ^{238}U (Ragetti et al., 1994; beige dot) are given for comparison. Errors for AVCC correction include uncertainties on AVCC composition. Error bars represent 1 σ.

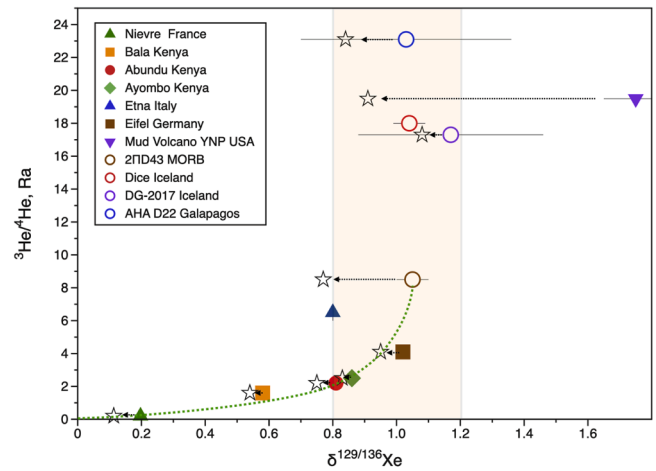

Fig. 8. Compilation of $\delta^{129/136}$Xe values for selected samples, as a function of the respective ^{3}He/^{4}He ratios (expressed as multiples of the atmospheric value Ra of 1.39×10^{-6}). $\delta^{129/136}$Xe stands for the $\delta^{129/130}$Xe/$\delta^{136/130}$Xe ratio. The filled symbols are gas samples analyzed by dynamic mass spectrometry (DMS) and the open symbols are rock samples analyzed by static mass spectrometry (SMS). Open stars represent data corrected for either isotope fractionation (gas samples) or chondritic (AVCC) contribution (rock samples) using published excesses of ^{128}Xe relative to the atmospheric composition ($\delta^{128/130}$Xe > 0 for gas samples). Corrected and non-corrected values are given in Table S1 (Supplementary Materials). Note that correction of gas data for either AVCC or isotope fractionation leads to similar values (Fig. 5). Nièvre is a CO_2-rich gas from exploration drilling in Nièvre County, France (Cardoso et al., 2023); Bala, Abundu, Ayombo are CO_2-rich gases from Homa Hills, Kenya (this work); Eifel stands for Victoriaquelle spring, a mineral spring gas from Miocene-Quaternary volcanic province in Germany (Bekaert et al., 2024); Etna is CO_2 gas from a drilling close to Mount Etna, Italy (Bekaert et al., 2024); Mud Volcano is a CO_2-rich bubble gas sample from the Mud Volcano area, Yellowstone National Park, USA (Bekaert et al., 2023); 2ПD43 is a mid-ocean ridge gas-rich sample often considered as a reference for the convective mantle sampled by MORBs (Péron and Moreira, 2018); DICE is subglacial gas-rich sample from the Icelandic mantle plume (Mukhopadhyay, 2012); DG-2017 is a subglacial glass from presumably the same sampling site as the DICE sample (Péron et al., 2021); AHA-NEMO2-D22 is a submarine basalt glass from the Galapagos mantle plume region (Péron et al., 2021). All samples but Nièvre and Bala display comparable $\delta^{129/136}$Xe within 1.0±0.2, despite having ^{3}He/^{4}He ratios spanning over one order of magnitude. The dotted green curve represents mixing between a crustal pole, defined as $\delta^{129/136}$Xe = 0 (no mantle ^{129}Xe), ^{3}He/^{4}He = 0.02 Ra, and a convective mantle pole, with $\delta^{129/136}$Xe = 1.05 (for the popping rock) and ^{3}He/^{4}He = 8 Ra. The best fit is obtained for a crustal endmember richer in ^{4}He (relative to ^{136}Xe*) than the mantle counterpart. This difference could be due to ^{4}He being preferentially released from crustal minerals compared to fissiogenic ^{136}Xe*.

production would also have triggered degassing of mantle noble gases including ^{129}Xe*. The initial ratios of Xe-producing isotopes, ^{129}I/^{244}Pu/^{238}U were about 360/9/1 (computed for present-day I = 10 ppb; Déruelle et al., 1992; U = 20 ppb; McDonough and Sun, 1995; and chondritic Pu/U = 0.0068; Hudson et al., 1989). Given the predominance of I and Pu relative to U, fine tuning of models of terrestrial degassing may potentially provide consistent solutions to account for the modern ^{129}Xe/^{136}Xe$_U$ and ^{136}Xe$_{Pu}$/^{136}Xe$_U$ ratios of about 1 and ≤ 0.1, respectively, observed in mantle-derived gases. Hence, the $\delta^{129/136}$Xe ratio has the potential to be a cumulative tracer of past mantle evolution. For instance, isolated mantle regions like the source of mantle plumes or the subcontinental lithospheric mantle should be characterized by specific $\delta^{129/136}$Xe ratios, affected by high ^{136}Xe$_{Pu}$* and ^{136}Xe$_U$*, respectively, as can be oberved from ^{3}He/^{4}He and ^{20}Ne/^{21}Ne systematics (Mukhopadhyay and Parai, 2019, and refs. therein).

In Fig. 8 we compare variations of the $\delta^{129/136}$Xe values with those of the associated ^{3}He/^{4}He ratios. For the Homa Hills samples, both ratios correlate (Fig. 8) which can be regarded as contribution of radiogenic/nucleogenic isotopes from the Archean crust to a common mantle component rich in ^{129}Xe*. The Homa Hills samples also show correlated variations between $\delta^{129/136}$Xe and Ar and N isotopic ratios (Fig. S1), that support contribution of radiogenic/fissiogenic noble gas isotopes from the underlying Archean crust to magmatic gas from the convecting mantle through the rifting system. Ayombo, which has a $\delta^{129/136}$Xe ratio close to the range of MORBs (Fig. 8), is the most pristine sample available in the Homa Hills region, even if its ^{3}He/^{4}He is significantly lower than MORB's. Ayombo gas may therefore be representative of mantle-derived volatiles in a rifting environment. In line with this view, we note that a MORB mantle origin was proposed for CO_2-rich gases from the Eifel volcanic province (Rhine graben rifting; Bekaert et al., (2024) and for gases sampled at Oldoinyo Lengai, a carbonatitic volcano located further south in the East African rift system (Fischer et al., 2009). Likewise, Mount Etna has a $\delta^{129/136}$Xe value similar to Ayombo and MORBs.

Gases from Etna, Eifel and Homa Hills have MORB-like Ne and all show low, if any, Xe$_{Pu}$ contribution compared to Xe$_U$. The picture emerging from these comparisons is that the convecting mantle, sampled by the Popping rock on one hand, and the Eifel, Etna and Ayombo gases on another hand, is rather homogeneous for $\delta^{129/136}$Xe ratios. Including data from a CO_2-rich gas sampled in Nièvre (France), which shows the lowest $\delta^{129/136}$Xe value among gases analyzed by DMS so far, we derive a mixing curve between a pure crustal end-member and

a MORB-like component that reasonably fits continental DMS data (Fig. 8). The best fit is obtained for a curvature parameter of 0.1 (Supplementary Materials). This implies that the crustal end-member is richer in ^{4}He, relative to fissiogenic Xe*, than the mantle end-member. Helium isotope ratios increase at a slower rate than the $\delta^{129/136}$Xe values, suggesting more efficient release of radiogenic He – compared to fissiogenic Xe – from crustal minerals. In contrast, the Ne isotope ratios of Kenya, Etna and Eifel gases are MORB-like, implying that nucleogenic Ne may be better retained in crustal minerals than He and Xe. The release efficiency may therefore be of the order of He>Xe>Ne and radiogenic/fissiogenic Xe isotopes may be new tool for evaluating the release of noble gases from rocks and minerals. It is not clear however why fissiogenic Xe would be more easily released than nucleogenic Ne, a point that may deserve detailed insight into production/release processes.

The case of the mantle plume signature deserves further investigation. A compilation of available high-precision (DMS) gas data together with mantle-derived rock data (analyzed by static mass spectrometry; SMS) shows surprisingly constant $\delta^{129/136}$Xe despite highly variable ^{3}He/^{4}He (Fig. 8). The Popping Rock sample (2ΠD43) characterizing the MORB reservoir fed by the convecting mantle (Péron and Moreira, 2018; Parai and Mukhopadhyay, 2021), glasses from the Galapagos and Iceland mantle plumes (Mukhopadhyay, 2012; Péron et al., 2021), geothermal gas from the Yellowstone mantle plume (Bekaert et al., 2023) and gases from volcanic provinces in continental settings (Germany, Etna, Italy, Kenya) all display comparable $\delta^{129/136}$Xe values within ~20 %, while corresponding ^{3}He/^{4}He vary over one order of magnitude (Fig. 8). The most puzzling observation is the $\delta^{129/136}$Xe ratios of mantle plume gases appears to be similar to those of gases associated with the convecting mantle while ^{3}He/^{4}He ratios vary by one order of magnitude. Likewise, the slopes of neon three isotope correlations change drastically between the convecting mantle composition (sampled by MORBs or gases from Mt. Etna, Eifel and Homa hills) and mantle plumes (characterized by Galapagos, Iceland and Yellowstone (Byrne et al, in press) gases). Hence this compilation of data shows a puzzling decoupling between light noble gas (He and Ne) and Xe isotopes.

The problem is even more acute when considering the respective proportions of fissiogenic Xe from ^{244}Pu (Xe_{Pu}) and ^{238}U (Xe_{U}). So far, available high precision dynamic mass spectrometry (DMS) data have shown very limited, if any, Xe_{Pu} compared to Xe_{U} (Bekaert et al., 2024; this work) while static mass spectrometry (SMS) data indicate significant Xe_{Pu} contributions, with for example a prominent proportion of Xe_{Pu} in Icelandic samples (Mukhopadhyay, 2012). This discrepancy is observed for convecting mantle samples (popping rock vs. Eifel and Homa Hills gases) as well as for mantle plume samples (DICE from Iceland vs. Yellowstone gas). One possibility is that this discrepancy could have an analytical origin, as the lower precision of SMS compared to DMS may obscure the real origin of fissiogenic Xe in mantle-derived rocks. Alternatively, these differences may reflect mantle heterogeneities that are not yet seen in the limited number of DMS gas data. If further DMS data confirm the low proportion of Xe_{Pu} across the different mantle domains, then the classical model of noble gas geochemistry may require revision: degassing of Xe_{Pu} would invariably require large scale mantle convection (Bekaert et al., 2024) that would not be limited to the present-day convecting mantle but should also involve mantle plume regions such that preserving He and Ne isotopic differences between these mantle domains would become problematic. Furthermore, how could the $\delta^{129/136}$Xe be near-constant if the fraction of Xe_{Pu} is so variable? The amount of Xe_{U} would also be expected to be variable between plumes and the MORB mantle domains due to contrasted U content and noble gas residence time. As of today, we see no clear solution to this conundrum. One promising line of research will be to consider whole mantle conection homogenizing Xe isotopes with He and Ne leaking from the core (Mundl et al., 2017; Bouhifd et al., 2019) and mixing up with recycled noble gases in the mantle source of plumes. This conundrum opens up new exciting areas of investigation, potentially requiring a major revision of geodynamical concepts as well as fine modelling, which is out of the scope of the present contribution.

4. Conclusion

We report new high precision data for geothermal noble gases sampled at Homa Hills, a rifting area of Kenya. Large quantities of gases were sampled following the Giggenbach method and noble gases (Ar, Kr, Xe) were analyzed by dynamic mass spectrometry (DMS), allowing a precision one to two orders of magnitude better than conventional noble gas static mass spectrometry (SMS). We analyzed neon isotopes by SMS and results are consistent with a convecting mantle origin for parent magmas. The analysis of nitrogen isotopologues allowed us to constrain the extent of atmospheric contamination of the samples.

Xenon isotope data, normalized to ^{130}Xe and atmospheric composition, display clear excesses of ^{129}Xe and $^{131\text{-}136}$Xe due to the decay of extinct ^{129}I and to the fission of extant ^{238}U and/or extinct ^{244}Pu, respectively. Component analysis points to the lack of ^{244}Pu fission products, all fissiogenic Xe being due to ^{238}U within errors. These results, in line with recent data for Eifel and Etna volcanic areas (Bekaert et al., 2024), require the ancient mantle to have been degassed early due to Hadean crustal production and Xe degassing in the ancient atmosphere.

Data show slight excesses of ^{128}Xe, for which a comparison with Kr isotope data suggests that these excesses are not due to subsurface isotopic fractionation otherwise often detected in natural gases worldwide (Bekaert et al., 2023). These excesses likely originated in the mantle, signaling residual chondritic Xe, or recycling of a paleo-atmospheric Xe component older than 2.4 Ga. The latter possibility would also have important outcome for the evolution of the Earth-atmosphere system.

The $\delta^{129/136}$Xe values show correlated variations with He and N isotope ratios that are consistent with contribution of crustal gases to a MORB-like component. In contrast the^{129}Xe*/^{136}Xe* ratios are surprisingly constant (within 20 % of each other) among gases from different mantle domains (i.e., mantle plumes vs. convective mantle) despite drastic variations of the associated ^{3}He/^{4}He ratios over one order of magnitude. Variations observed in the present samples are likely due to appear to be due to differential crustal contribution. The contrasted behavior of Xe compared to He and Ne isotope systems may require reconsideration of models of terrestrial degassing and mantle convection.

CRediT authorship contribution statement

B. Marty: Writing – review & editing, Writing – original draft, Resources, Project administration, Methodology, Investigation, Funding acquisition, Formal analysis, Conceptualization. **D. Contamine:** Writing – original draft, Methodology, Investigation, Formal analysis. **D.V. Bekaert:** Writing – review & editing, Writing – original draft, Methodology, Investigation. **A. Lastes:** Writing – original draft, Investigation, Formal analysis. **R. Pik:** Investigation. **J. Labidi:** Writing – original draft, Formal analysis, Data curation. **E.D. Young:** Formal analysis. **M. W. Broadley:** Writing – review & editing, Writing – original draft, Investigation. **P.H. Barry:** Writing – review & editing, Writing – original draft, Investigation. **D.J. Byrne:** Writing – review & editing, Formal analysis. **A.M. Seltzer:** Writing – review & editing, Writing – original draft, Methodology, Investigation, Formal analysis, Data curation.

Declaration of competing interest

The authors declare the following financial interests/personal relationships which may be considered as potential competing interests: Bernard Marty reports a relationship with UL University that includes: employment, funding grants, and travel reimbursement. If there are other authors, they declare that they have no known competing financial

interests or personal relationships that could have appeared to influence the work reported in this paper.

Acknowledgements

We thank Yves Géraud, Jacques Varet, Peter Omenda, Marc Diraison, and Bastien Walter for logistical support and help during field work done in the framework of the EU-supported "Geothermal village" project. Laboratory assistance was provided by Laurent Zimmermann, as always. We thank editor Fang-Zen Teng for efficiency and two anonymous reviewers for helpful and constructive comments. This work was partially by the European Research Council Grant 695618 to B.M. We acknowledge NSF awards 2121637, 2152551 and 2319897 to PHB and 2151120 to PHB, AMS and DVB. MWB acknowledges support from NERC grant NE/X01732X/1.

Supplementary materials

Supplementary material associated with this article can be found, in the online version, at doi:10.1016/j.epsl.2025.119224.

Data availability

Data will be made available on request.

References

Alexander Jr, E.C., Lewis, R.S., Reynolds, J.H., Michel, M.C., 1971. Plutonium-244: Confirmation as an extinct radioactivity. Science 172, 837–840.

Aka, F.T., Kusakabe, M., Nagao, K., Tanyileke, G., 2001. Noble gas isotopic compositions and water/gas chemistry of soda springs from the islands of Bioko, São Tomé and Annobon, along with Cameroon Volcanic Line. West Africa. Appl. Geochem. 16, 323–338. https://doi.org/10.1016/S0883-2927(00)00037-8.

Ardoin, L., Broadley, M.W., Almayrac, M., Avice, G., Byrne, D.J., Tarantola, A., Lepland, A., Saito, T., Komiya, T., Shibuya, T., Marty, B., 2022. The end of the isotopic evolution of atmospheric xenon. Geochem. Persp. Lett. 20, 43–47. https://doi.org/10.7185/geochemlet.2207.

Avice, G., Marty, B., Burgess, R., 2017. The origin and degassing history of the Earth's atmosphere revealed by Archean xenon. Nat. Comm. 8, 15455. https://doi.org/10.1038/ncomms15455.

Avice, G., Marty, B., Burgess, R., Hofmann, A., Philippot, P., Zahnle, K., Zakharov, D., 2018. Evolution of atmospheric xenon and other noble gases inferred from Archean to Paleoproterozoic rocks. Geochim. Cosmochim. Acta 232, 82–100. https://doi.org/10.1016/j.gca.2018.04.018.

Bekaert, D.V., Barry, P.H., Broadley, M.W., Byrne, D.J., Marty, B., Ramírez, C.J., De Moor, J.M., Rodriguez, A., Hudak, M.R., Subhas, A.V., Halldórsson, S.A., Stefánsson, A., Caracausi, A., Lloyd, K.G., Giovannelli, D., Seltzer, A.M., 2023. Ultrahigh-precision noble gas isotope analyses reveal pervasive subsurface fractionation in hydrothermal systems. Sci. Adv. 9. https://doi.org/10.1126/sciadv.adg2566 eadg2566.

Bekaert, D.V., Broadley, M.W., Caracausi, A., Marty, B., 2019. Novel insights into the degassing history of Earth's mantle from high precision noble gas analysis of magmatic gas. Earth Planet. Sci. Lett. 525, 115766. https://doi.org/10.1016/j.epsl.2019.115766.

Bekaert, D.V., Caracausi, A., Marty, B., Byrne, D.J., Broadley, M.W., Caro, G., Barry, P.H., Seltzer, A.M., 2024. The low primordial heavy noble gas and ^{244}Pu-derived Xe contents of Earth's convecting mantle. Earth Planet. Sci. Lett. 642, 118886. https://doi.org/10.1016/j.epsl.2024.118886.

Bekaert, D.V., Turner, S.J., Broadley, M.W., Barnes, J.D., Halldórsson, S.A., Labidi, J., Wade, J., Walowski, K.J., Barry, P.H., 2021. Subduction-Driven Volatile Recycling: A Global Mass Balance. Annu. Rev. Earth Planet. Sci. 49, 37–70. https://doi.org/10.1146/annurev-earth-071620-055024.

Bouhifd, M.A., Jephcoat, A.P., Porcelli, D., Kelley, S.P., Marty, B., 2019. Potential of Earth's core as a reservoir for noble gases: case for helium and neon. Geochem. Persp. Lett. 15. https://doi.org/10.7185/geochemlet.2028.

Broadley, M.W., Barry, P.H., Bekaert, D.V., Byrne, D.J., Caracausi, A., Ballentine, C.J., Marty, B., 2020. Identification of chondritic krypton and xenon in Yellowstone gases and the timing of terrestrial volatile accretion. Proceed. Nat. Acad. Sci. 117, 13997–14004. https://doi.org/10.1073/pnas.2003907117.

Butler, W.A., Jeffery, P.M., Reynolds, J.H., Wasserburg, G.J., 1963. Isotopic variations in terrestrial gases. J. Geophys. Res. 68, 3283–3291.

Cardoso, C.D., Russier, E., Marty, B., Pik, R., Bekaert, D.V., Seltzer, A., Broadley, M.W., Byrne, D., Rigaudier, T., Géraud, Y., Tarantola, A., Hauville, B., 2023. Helium isotope evidence for cryptic magmatism along central France. Chem. Geol 634, 121588.

Cartigny, P., Marty, B., 2013. Nitrogen Isotopes and Mantle Geodynamics: The Emergence of Life and the Atmosphere-Crust-Mantle Connection. Elements 9, 359–366. https://doi.org/10.2113/gselements.9.5.359.

Chorowicz, J., 2005. The East African rift system. J. African Earth Sci. 43, 379–410. https://doi.org/10.1016/j.jafrearsci.2005.07.019.

Coltice, N., Marty, B., Yokochi, R., 2009. Xenon isotope constraints on the thermal evolution of the early Earth. Chem. Geol. 266, 4–9. https://doi.org/10.1016/j.chemgeo.2009.04.017.

Darling, W.G., Griesshaber, E., Andrews, J.N., Armannson, H., O'Nions, R.K., 1995. The origin of hydrothermal helium and other rare gases in the Kenya Rift Valley. Geochim. Cosmochim. Acta 59, 2501–2512.

Fischer, T.P., Burnard, P., Marty, B., Hilton, D.R., Furi, E., Palhol, F., Sharp, Z.D., Mangasini, F., 2009. Upper-mantle volatile chemistry at Oldoinyo Lengai volcano and the origin of carbonatites. Nature 459, 77–80. https://doi.org/10.1038/nature07977.

Foley, S.F., Link, K., Tiberindwa, J.V., Barifaijo, E., 2012. Patterns and origin of igneous activity around the Tanzanian craton. J. African Earth Sci. 62, 1–18. https://doi.org/10.1016/j.jafrearsci.2011.10.001.

Giggenbach, W.F., 1975. A simple method for the collection and analysis of volcanic gas samples. Bull. Volcanol. 39, 132–145. https://doi.org/10.1007/BF02596953.

Giggenbach, W.F., 1980. Geothermal gas equilibria. Geochim. Cosmochim. Acta 44, 2021–2032.

Gilfillan, S.M.V., Györe, D., Flude, S., Johnson, G., Bond, C.E., Hicks, N., Lister, R., Jones, D.G., Kremer, Y., Haszeldine, R.S., Stuart, F.M., 2019. Noble gases confirm plume-related mantle degassing beneath Southern Africa. Nat Comm 10, 5028. https://doi.org/10.1038/s41467-019-12944-6.

Déruelle, B., Dreibus, G., Jambon, A., 1992. Iodine abundances in oceanic basalts: Implications for Earth Dynamics. Earth Planet. Sci. Lett. 108, 217–227.

Halldórsson, S.A., Hilton, D.R., Scarsi, P., Abebe, T., Hopp, J., 2014. A common mantle plume source beneath the entire East African Rift System revealed by coupled helium-neon systematics. Geoph. Res. Lett. 41, 2304–2311. https://doi.org/10.1002/2014GL059424.

Hébrard, E., Marty, B., 2014. Coupled noble gas – hydrocarbon evolution of the early Earth atmosphere upon solar UV irradiation. Earth Planet. Sci. Lett. 385, 40–48. https://doi.org/10.1016/j.epsl.2013.10.022.

Holland, G., Ballentine, C.J., 2006. Seawater subduction controls the heavy noble gas composition of the mantle. Nature 441, 186–191.

Holland, G., Cassidy, M., Ballentine, C., 2009. Meteorite Kr in Earth's Mantle. Science 326, 1522–1526.

Hudson, G.B., Kennedy, B.M., Podosek, F.A., Hohenberg, C.M., 1989. The early solar system abundance of ^{244}Pu as interred from the St. Severin chondrite. In: Proceedings of the 19th Lunar and Planetary Science Conference. Lunar and Planetary Institute, pp. 547–557.

Japan International Cooperation Agency Report, 1990. Report on the mineral exploration in the Homa Bay area. Republic of Kenya (open report). https://openjicareport.jica.go.jp/pdf/10800324_01.pdf.

Kobayashi, M., Sumino, H., Nagao, K., Ishimaru, S., Arai, S., Yoshikawa, M., Kawamoto, T., Kumagai, Y., Kobayashi, T., Burgess, R., Ballentine, C.J., 2017. Slab-derived halogens and noble gases illuminate closed system processes controlling volatile element transport into the mantle wedge. Earth Planet. Sci. Lett. 457, 106–116. https://doi.org/10.1016/j.epsl.2016.10.012.

Kunz, J., Staudacher, T., Allègre, C.J., 1998. Plutonium-fission xenon found in the Earth's mantle. Science 280, 877–880.

Labidi, J., Barry, P.H., Bekaert, D.V., Broadley, M.W., Marty, B., Giunta, T., Warr, O., Sherwood Lollar, B., Fischer, T.P., Avice, G., Caracausi, A., Ballentine, C.J., Halldórsson, S.A., Stefánsson, A., Kurz, M.D., Kohl, I.E., Young, E.D., 2020. Hydrothermal $^{15}N^{15}N$ abundances constrain the origins of mantle nitrogen. Nature 580, 367–371. https://doi.org/10.1038/s41586-020-2173-4.

Labidi, J., Young, E.D., 2022. The origin and dynamics of nitrogen in the Earth's mantle constrained by $^{15}N^{15}N$ in hydrothermal gases. Chem. Geol. 591, 120709. https://doi.org/10.1016/j.chemgeo.2022.120709.

Labidi, J., Young, E.D., Fischer, T.P., Barry, P.H., Ballentine, C.J., de Moor, J.M., 2021. Recycling of nitrogen and light noble gases in the Central American subduction zone: constraints from $^{15}N^{15}N$. Earth Planet. Sci. Lett. 571, 117112. https://doi.org/10.1016/j.epsl.2021.117112.

Lee, J.Y., Marti, K., Severinghaus, J.P., Kawamura, K., Yoo, H.S., Lee, J.B., Kim, J.S., 2006. A redetermination of the isotopic abundances of atmospheric Ar. Geochim. Cosmochim. Acta 70, 4507–4512. https://doi.org/10.1016/j.gca.2006.06.1563.

Mabry, J., Lan, T., Burnard, P., Marty, B., 2013. High-precision helium isotope measurements in air. J. Anal. Atom. Spectrom. 28. https://doi.org/10.1039/c3ja50155h.

Mamyrin, B.A., Tolstikhin, I.N., 1984. Helium Isotopes in Nature. Elsevier.

Marty, B., 1984. On the Noble-Gas Isotopic Fractionation in Naturally-Occurring Gases. Geochem. J. 18, 157–162.

Marty, B., Tolstikhin, I., Kamensky, I.L., Nivin, V., Balaganskaya, E., Zimmermann, J.L., 1998. Plume-derived rare gases in 380 Ma carbonatites from the Kola region (Russia) and the argon isotopic composition in the deep mantle. Earth Planet. Sci. Lett. 164, 179–192.

Marty, B., Almayrac, M., Barry, P.H., Bekaert, D.V., Broadley, M.W., Byrne, D.J., Ballentine, C.J., Caracausi, A., 2020. An evaluation of the C/N ratio of the mantle from natural CO_2-rich gas analysis: Geochemical and cosmochemical implications. Earth Planet. Sci. Lett. 551, 116574. https://doi.org/10.1016/j.epsl.2020.116574.

Mazor, E., Heymann, D., Anders, E., 1970. Noble gases in carbonaceous chondrites. Geochim. Cosmochim. Acta 34, 781–824.

McDonough, W.F., Sun, S.S., 1995. The composition of the Earth. Chem. Geol. 120, 223–253.

Moreira, M., Kunz, J., Allègre, C.J., 1998. Rare gas systematics in Popping Rock: Isotopic and elemental compositions in the upper mantle. Science 279, 1178–1181.

Mukhopadhyay, S., 2012. Early differentiation and volatile accretion recorded in deep-mantle neon and xenon. Nature 486, 101–104. https://doi.org/10.1038/nature11141.

Mukhopadhyay, S., Parai, R., 2019. Noble Gases: A Record of Earth's Evolution and Mantle Dynamics. Annu. Rev. Earth Planet. Sci. 47, 389–419. https://doi.org/10.1146/annurev-earth-053018-060238.

Mundl, A., Touboul, M., Jackson, M.G., Day, J.M.D., Kurz, M.D., Lekic, V., Helz, R.T., Walker, R.J., 2017. Tungsten-182 heterogeneity in modern ocean island basalts. Science 356, 66–69.

Nagao, K., Takaoka, N., Matsubayashi, O., 1979. Isotopic anomalies of rare-gases in the Nigorikawa Geothermal Area, Hokkaido, Japan. Earth Planet. Sci. Lett. 44, 82–90.

Ozima, M., Podosek, F.A., 2002. Noble gas geochemistry. Cambridge University Press, Cambridge.

Ozima, M., Podosek, F.A., Igarashi, G., 1985. Terrestrial xenon isotope constraints on the early history of the Earth. Nature 315, 471–474.

Parai, R., Mukhopadhyay, S., 2021. Heavy noble gas signatures of the North Atlantic Popping Rock 2ΠD43: Implications for mantle noble gas heterogeneity. Geochim. Cosmochim. Acta 294, 89–105. https://doi.org/10.1016/j.gca.2020.11.011.

Parai, R., Mukhopadhyay, S., 2018. Xenon isotopic constraints on the history of volatile recycling into the mantle. Nature 560, 223–227. https://doi.org/10.1038/s41586-018-0388-4.

Pepin, R.O., 2006. Atmospheres on the terrestrial planets: Clues to origin and evolution. Earth Planet. Sci. Lett. 252, 1–14. https://doi.org/10.1016/j.epsl.2006.09.014.

Pepin, R.O., Porcelli, D., 2006. Xenon isotope systematics, giant impacts, and mantle degassing on the Ealy Earth. Earth Planet. Sci. Lett. 250, 470–485.

Péron, S., Moreira, M., 2018. Onset of volatile recycling into the mantle determined by xenon anomalies. Geochem. Persp. Lett. 9, 21–25. https://doi.org/10.7185/geochemlet.1833.

Péron, S., Mukhopadhyay, S., Kurz, M.D., Graham, D.W., 2021. Deep-mantle krypton reveals Earth's early accretion of carbonaceous matter. Nature 600, 462–467. https://doi.org/10.1038/s41586-021-04092-z.

Piani, L., Marrocchi, Y., Rigaudier, T., Vacher, L.G., Thomassin, D., Marty, B., 2020. Earth's water may have been inherited from material similar to enstatite chondrite meteorites. Science 369, 1110–1113. https://doi.org/10.1126/science.aba1948.

Pujol, M., Marty, B., Burgess, R., 2011. Chondritic-like xenon trapped in Archean rocks: A possible signature of the ancient atmosphere. Earth Planet. Sci. Lett. 308, 298–306. https://doi.org/10.1016/j.epsl.2011.05.053.

Ragettli, R.A., Hebeda, E.H., Signer, P., Wieler, R., 1994. Uranium-xenon chronology: precise determination of λsf* 136Ysf for spontaneous fission of ^{238}U. Earth Planet. Sci. Lett. 128, 653–670.

Seltzer, A.M., Bekaert, D.V., 2022. A unified method for measuring noble gas isotope ratios in air, water, and volcanic gases via dynamic mass spectrometry. Int. J. Mass Spectrom. 478, 116873. https://doi.org/10.1016/j.ijms.2022.116873.

Severinghaus, J.P., Bender, M.L., Keeling, R.F., Broecker, W.S., 1996. Fractionation of soil gases by diffusion of water vapor, gravitational settling, and thermal diffusion. Geochim. Cosmochim. Acta 60, 1005–1018. https://doi.org/10.1016/0016-7037(96)00011-7.

Sumino, H., Burgess, R., Mizukami, T., Wallis, S.R., Holland, G., Ballentine, C.J., 2010. Seawater-derived noble gases and halogens preserved in exhumed mantle wedge peridotite. Earth Planet. Sci. Lett. 294, 163–172.

Tole, M.P., 1988. Low enthalpy geothermal systems in Kenya. Geothermics 17, 777–783. https://doi.org/10.1016/0375-6505(88)90037-5.

Turner, G., Busfield, A., Crowther, S. A., Harrison, M., Mojzsis, S. J., & Gilmour, J., 2007. Pu–Xe, U–Xe, U–Pb chronology and isotope systematics of ancient zircons from Western Australia. Earth Planet. Sci. Lett. 261, 491-499.

Vermeesch, P., 2018. IsoplotR: A free and open toolbox for geochronology. Geosci. Front. 9, 1479–1493. https://doi.org/10.1016/j.gsf.2018.04.001.

Yeung, L.Y., Li, S., Kohl, I.E., Haslun, J.A., Ostrom, N.E., Hu, H., Fischer, T.P., Schauble, E.A., Young, E.D., 2017. Extreme enrichment in atmospheric ^{15}N^{15}N. Sci. Adv. 3, eaao6741.

Yokochi, R., Marty, B., 2005. Geochemical constraints on mantle dynamics in the Hadean. Earth Planet. Sci. Lett. 238, 17–30.

Young, E.D., Galy, A., Nagahara, H., 2002. Kinetic and equilibrium mass-dependant isotope fractionation laws in nature and their geochemical and cosmochemical significance. Geochim. Cosmochim. Acta 66, 1095–1104. https://doi.org/10.1016/S0016-7037(01)00832-8.

Zahnle, K.J., Gacesa, M., Catling, D.C., 2019. Strange messenger: A new history of hydrogen on Earth, as told by Xenon. Geochim. Cosmochim. Acta 244, 56–85. https://doi.org/10.1016/j.gca.2018.09.017.